Numerical heat transfer model for swelling intumescent coatings during heating

Andrea Lucherini[1,2,3*], Juan P. Hidalgo[2], Jose L. Torero[4], and Cristian Maluk[2,5]

[1] School of Civil Engineering, The University of Queensland, Australia.

[2] Department of Structural Engineering and Building Materials, Ghent University, Belgium.

[3] Department for Fire-safe Sustainable Built Environment (FRISSBE), Slovenian National Building and Civil Engineering Institute (ZAG), Ljubljana, Slovenia.

[4] Department of Civil, Environmental & Geomatic Engineering, University College London, UK.

[5] Astute Fire, London, UK.

[*] Corresponding author: Dr Andrea Lucherini, Sint-Pietersnieuwstraat 41, 9000 Ghent, Belgium. ORCID: 0000-0001-8738- 1018. Email address: Andrea.Lucherini@UGent.be.

ABSTRACT

This research study presents a heat transfer model aimed at estimating the thermal and physical response of intumescent coatings. The numerical model is inspired by the outcomes of an experimental study focused on analysing the insulating effectiveness of a commercial intumescent coating for a range of heating conditions and initial coating thickness. The model solves the one-dimensional heat conduction problem using the finite-difference Crank-Nicolson method, and it assumes that the effectiveness of intumescent coatings is mainly dependent on their ability to develop swelled porous char. The coating swelling is implemented in the model by adopting an approach based on expanding the mesh representing the physical domain in proximity to the substrate-coating interface. The model described herein offers researchers and engineers a tool to estimate the heat transfer of swelling intumescent coatings (i.e. in-depth thermal gradient). Outcomes of the analysis shown herein demonstrate that the heat conduction within intumescent coatings is governed by the physical coating swelling and the thermal conditions at the coating-substrate interface. The numerical model shows that its accuracy is highly influenced by the coating thickness ahead of the reaction zone. Consequently, the coating swelling rate plays a key role, while the thermo-physical properties of the intumescent coating have a secondary effect. According to its assumptions, the model defines a quasi-steady-state thermal problem: it is more accurate for conditions close to steady-state (e.g. high heat fluxes), but it loses accuracy for cases characterised by transient phenomena (e.g. phases prior to the onset of swelling and low heat fluxes).

KEYWORDS

Intumescent coatings; heat transfer; numerical model; swelling; fire safety.

1 INTRODUCTION AND BACKGROUND

In recent times, various fire safety solutions have become a common practice to ensure the stability and integrity of structural systems in the event of a fire. For example, the application of different thermal barriers characterised by low thermal conductivity, such as gypsum plaster-boards or cementitious spray-on systems, is a widely used method to limit the rate of temperature increase within structural elements exposed to fire [1]. Fundamentally different from conventional applications, intumescent coatings (also known as "reactive coatings") represent an innovative fire safety solution for protecting load-bearing structural steel systems during fire. Traditional solutions are usually deemed relatively inexpensive and easy to apply, but aesthetically unpleasant and undesirable for the modern slender structures with visible steelwork. The unique advantages of intumescent coatings, such as the attractive appearance of visible structures, lightweight, ease and flexibility for both on- and off-site applications, have fostered their success and extensive use worldwide [2-3]. Furthermore, the construction industry has been looking at the possibility of applying intumescent coatings to protect different substrate materials. For example, it was found that the application of intumescent coatings can mitigate the destructive effects of fire-induced concrete spalling, prevent surface ignition and reduce the charring rate of wooden elements [4-5].

Intumescent coatings are thermally reactive materials, usually composed of a combination of organic and inorganic components bound together in a polymer matrix [6]. At ambient temperature, these systems appear as a pigmented thin coating, applied to a Dry Film Thickness (DFT) in the order of few millimetres (thin intumescent coatings) or few centimetres (thick intumescent coatings). When exposed to heat, they can swell to form a thick, low-density and highly-insulating porous char that prevents the substrate material from reaching high temperatures that can compromise structural stability and integrity. Thin intumescent coatings can swell up to 100 times their initial thickness following typical reaction stages in the so-called "intumescent process" [7].

Over the past decades, the research community has extensively investigated the behaviour of intumescent coatings exposed to fire conditions and adopted different experimental methodologies to understand the effects of different factors on the swelling of intumescent coatings [7-8]. The final goal is to develop performance-based design methodologies to quantify the effectiveness of intumescent coatings as a thermal barrier for structural elements [9]. Since intumescent coatings are chemically-reactive materials, the research community has demonstrated that several factors influence the intumescent process and the overall insulation effectiveness: for instance, the heating exposure, the substrate thermal conditions and the applied initial thickness, as well as the chemical formulation [7, 10-18]. However, despite the complexity of the behaviour of these materials, the

insulating capacity of intumescent coatings is typically assessed based on a single exposure in standard furnace fire resistance tests [19-20]. In these tests, real-scale coated samples are exposed to the standard temperature-time fire curve and, based on the recorded temperatures, simplified engineering methods (e.g. tabulated fire ratings and effective thermal conductivity method) are commonly adopted for design purposes [21].

The swelling of intumescent coatings under heat is a phenomenon involving a complex combination of different material phases, mixtures and reactions. Many variables are extremely difficult to measure, and the intumescent process is hard to predict. Small-scale or large-scale experimental data can be used to describe the heat transfer and swelling process of intumescent coatings based on chemical kinetics, mass and energy conservation [14-15, 22-26].

Various numerical and mathematical models covering a range of complexities have been developed to simulate the swelling behaviour and the heat transfer through swelling intumescent coatings under thermal exposure [7]. However, due to the significant complexity and the wide range of products available in the market, researchers have followed different approaches and adopted various methodologies to investigate this topic [27]. The problem can be simplified in different ways, like identifying independent global chemical reactions (e.g. melting, swelling and charring) or subdividing the coating into independent components (e.g. solid char, pores and gas phase) [22, 28-29]. While these models have all been shown to have some predictive capacity, they all require many input parameters, of which some need to be derived from complex experimental data in an indirect manner, such as the coating melting temperature or the intumescent char porosity.

The complex and uncertain quantification of input parameters forces designers and researchers to rely on highly-simplified numerical models. The development of more precise models is primarily hindered by the lack of experimental studies that explicitly quantify the thermal (in-depth temperature gradient and surface temperature) and physical aspects (swelled coating thickness) of swelling intumescent coatings during the thermal exposure [7]. These features are usually only implicitly considered, starting from the temperature evolution of the protected substrate material (typically steel).

The most common approach simply aims at predicting the temperature evolution of the substrate material (e.g. steel) protected by the intumescent coating. This problem is usually solved by treating the coating as an inert material (no swelling) and estimating effective material properties as an equivalent thermal barrier to the protected substrate. Typically, the majority of the thermal and physical properties of the intumescent coating are kept constant, while a temperature-dependent

thermal resistance or thermal conductivity is estimated [13, 18, 21, 30-32]. Consequently, the effective material properties do not correctly represent the thermo-physical response of intumescent coatings. As a result, these models show a high variance of the values reported in the literature; in a few studies, even values lower than the thermal conductivity of air were reported [7]. Similar approaches are also commonly used when adopting various commercial finite-element software (e.g. TNO-Diana, SAFIR and ABAQUS) to simulate the temperature evolutions and consequent failure modes of various protected structural elements exposed to fire [33-35].

Recent research studies proposed an experimental methodology aimed at analysing the effectiveness of intumescent coatings through a detailed characterisation of their thermal and physical response. This was obtained by measuring the evolution of the swelled coating thickness, the substrate and the coating surface temperatures, and the transient in-depth temperature profile [16]. Using the Heat-Transfer Rate Inducing System (H-TRIS) test method, uncoated and coated steel plates were tested using a movable array of radiant panels [16, 36-37]. The experimental outcomes offered an explicit understanding of how the heating conditions, the substrate thermal conditions and the applied initial coating thickness affect the behaviour of a commercial solvent-based thin intumescent coating. This product was already examined in other research investigations and it was demonstrated to have similar characteristics to typical intumescent formulations based on the APP-PER-MEL system [5, 7, 16-17, 38-41]. The experimental results also serve as the basis for developing a heat transfer model to analyse and simulate the temperature increase of uncoated and coated steel samples prior to the onset of swelling [40].

The objective of this research study is to propose a new heat transfer model based on the more precise measurements and well-defined boundary conditions. The heat transfer model presented herein is inspired by the above-mentioned experimental campaigns on intumescent-coated steel plates carried out by Lucherini *et al.* [16, 38, 40]. The numerical model offers an engineering tool to estimate the thermal gradient within swelling intumescent coatings and the temperature evolution of the coating surface and the protected substrate (i.e. steel). This covers a greater number of variables to previous models and a range of conditions and scenarios, in terms of heating conditions and applied initial coating thickness.

2 DESCRIPTION OF THE NUMERICAL HEAT MODEL

2.1 General approach and assumptions

The model focuses on solving the one-dimensional heat conduction problem (starting from the coating heated surface, through the swelling coating and towards the protected substrate material) by

resolving heat conservation equation for a non-reacting, non-porous opaque solid medium [42]. The heat conservation equation is solved using a finite-difference numerical model based on the Crank-Nicolson method, which is implicit in time, numerically stable and computationally efficient [43-44].

The physical domain is discretised into a single-layer material (intumescent coating only) with a total thickness equal to L, which corresponds to the actual coating thickness d_c (virgin or swelled). As shown in Figure 1, the material discretisation is organised into finite N elements represented by N nodes. The interior elements have the node placed in the element's centre, and they have a thickness of Δx. On the other hand, the boundary elements (surface element and end element) have the node placed at the element's edge, and they have a thickness of $\Delta x/2$. No interface elements are considered.

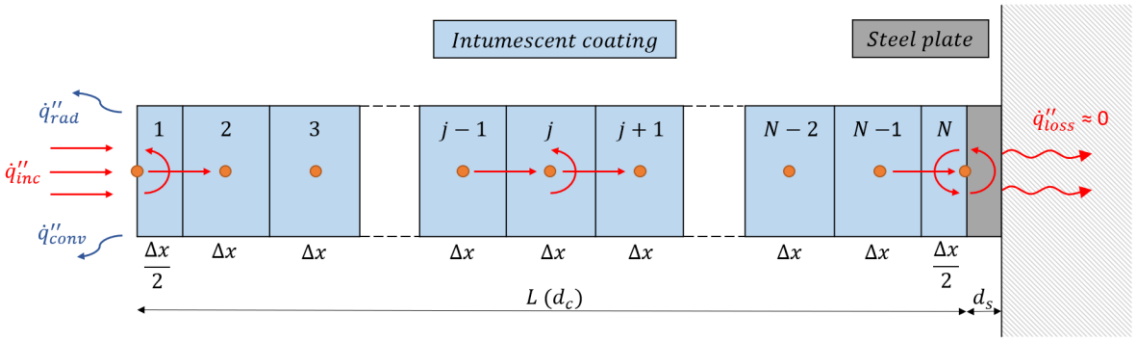

Figure 1. Schematic illustration of the single-layer material heat transfer model including the thermal boundary conditions.

The model relies on the accurate definition of the thermal conditions at the coating boundaries (refer to Figure 1). The thermal boundary condition at the exposed surface is defined by the time-history of incident radiant heat flux imposed by the H-TRIS test method ($\dot{q}''_{inc}$) with convective and radiative heat flux losses ($\dot{q}''_{conv}$ and $\dot{q}''_{rad}$) to the surrounding environment at ambient temperature [36-37]. The thermal boundary conditions are modelled using conventional correlations available in the literature [38, 42]. Since the unexposed surface of the coated steel plates was insulated using low thermal inertia materials, adiabatic conditions were assumed. Due to the thermally-thin nature of the substrate steel plate (low Biot number), it was lumped into a thermal mass connected to the coating end element. The coating end element is characterised by a single temperature, which corresponds to the same temperature of the steel-coating interface.

The experimental results emphasised how the swelling process and the resulting swelled thickness govern the thermal and physical response of intumescent coatings [16]. Accordingly, the model assumes that the insulating effectiveness of the thermal barrier provided by the intumescent coating is mainly dependent on the ability to develop swelled porous char. The intumescent coating is modelled as a swelling solid media with constant material properties. Due to the limited dimensions

and mass of the intumescent coating, the model does not include any heat generation/absorption (heat source term) within the material elements.

The swelling of the intumescent coating is modelled by increasing the thickness of the protective thermal barrier by adding finite elements to the coating discretisation, in particular in proximity to the substrate-coating interface. In this way, the protective thermal barrier developed by the intumescent coating increases its thickness during thermal exposure. Empirical correlations (discussed in Section 2.3) are introduced to describe the evolution of the swelled coating thickness during thermal exposure [16, 38].

Starting from the heat conservation equation at each node, thus each element, *N* linear equations with *N* variables (i.e. temperatures of each node at specific time step) can be defined. The defined system of equations forms a tridiagonal matrix system, which is solved to calculate the temperature evolution of each node for each time step. The detailed derivation of the governing equations and numerical heat transfer model can be found in [38].

2.2 Implementing the swelling of the intumescent coating

In accordance with the presented experimental outcomes [16], the swelling of intumescent coatings is implemented in the heat transfer model in a manner that the swelling reaction occurs in proximity to the substrate-coating interface, where the virgin coating is located and sustains the process. In this way, the swelling intumescent coating insulates the protected substrate by displacing the already-swelled coating toward the direction of the heat source. In other words, the thermal gradient within the intumescent coating is stretched from the substrate due to the coating swelling. This is the main reason why, when the swelling reaction is occurring, the protected substrate remains within the temperature range at which the intumescent coating typically undergoes the swelling reaction (300-400°C), while the substrate temperature increases above this threshold once the swelling process is completed [16, 38-39]. Accordingly, the swelling of the intumescent coating is modelled by adding finite elements of the same thickness Δx at the steel-coating interface, particularly next to the coating end element. Given the limited mass of the swelled coating compared to the initial system (virgin coating), mass conservation is not satisfied, but this aspect has little influence from a thermal perspective. The spatial discretisation Δx and time step Δt are defined small enough to accurately describe the coating swelling and avoid numerical instabilities. Figure 2 offers a schematic illustration of the modelling approach. Adaptive mesh (fixed *N* elements but increasing Δx) was not considered as a modelling option because it would not have correctly represented the physics observed in the experimental campaign.

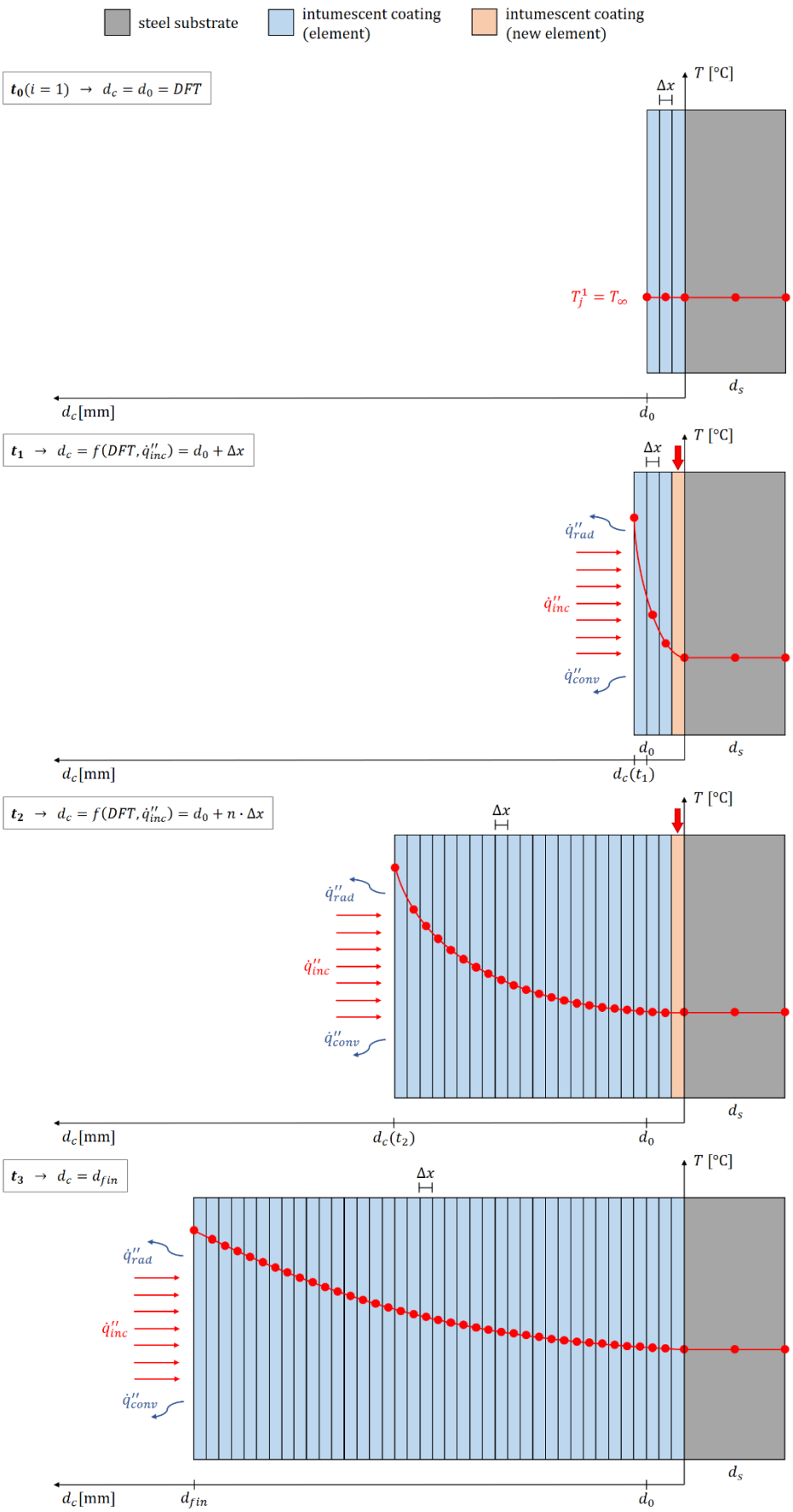

Figure 2. Schematic illustration of the heat transfer model formulated for swelling intumescent coatings.

The newly added element is introduced at the same temperature as the previous coating end element. The temperature of the new second-last coating element is calculated as the average value between the temperatures of the two adjacent elements. In this way, the protective thermal barrier developed by the intumescent coating increases its thickness during the thermal exposure following the empirical correlations defined in Section 2.3. Following this approach, the size of the tridiagonal matrix system to calculate the temperature evolution of each node for each time step continuously increases until the swelling reaction of the intumescent coating is completed.

2.3 Definition of the swelled coating thickness

The experimental campaign demonstrated that the incident heat flux governs the swelling rate of the intumescent coating, while the applied initial DFT governs the maximum swelled coating thickness that the intumescent coating could reach during the thermal exposure [16]. The empirical correlations shown in Figure 3 and Figure 4 were proposed to estimate the evolution of the swelled coating thickness during the thermal exposure, starting from a well-defined thermal boundary condition (i.e. incident heat flux) at the coating surface and the applied initial coating thickness [16].

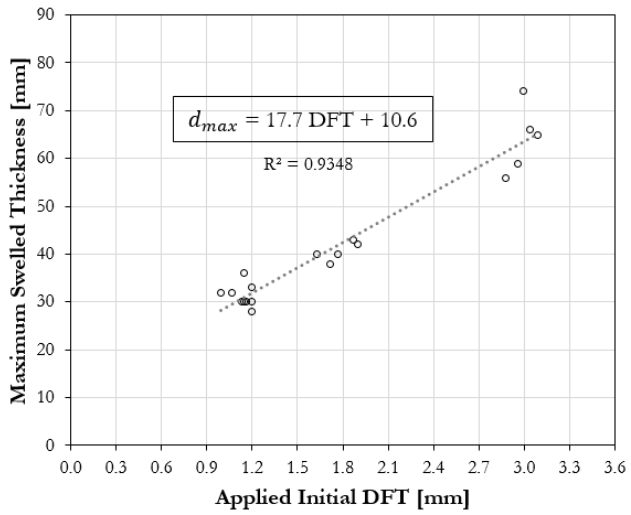

Figure 3. Empirical correlation for estimating the maximum swelled thickness of the intumescent coating as a function of the applied initial DFT.

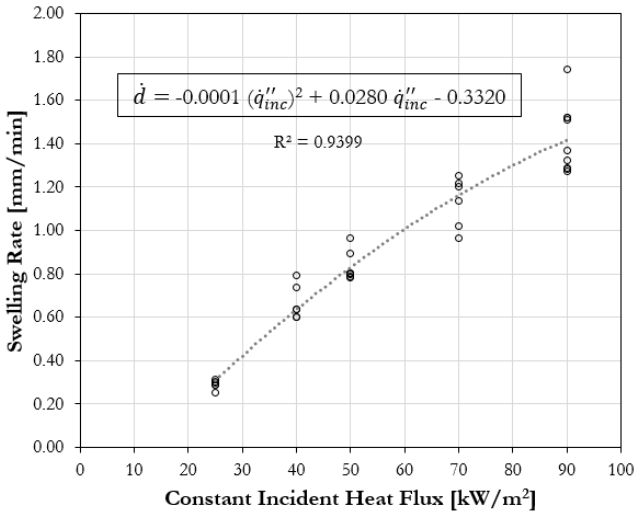

Figure 4. Empirical correlation for estimating the swelling rate of the intumescent coating as a function of the constant incident heat flux.

Accordingly, as shown in Figure 3, the maximum swelled coating thickness of the intumescent coating d_{max} [mm] can be expressed as a function of the applied initial *DFT* [mm]:

$$d_{max} = 17.7 \cdot DFT + 10.6 \quad (1)$$

The same experimental results evidenced how an empirical correlation can be used to link the constant incident heat flux and the swelling rate of the intumescent coating, as shown in Figure 4. Also, considering the outcomes presented by another research study, the same intumescent coating required

incident heat fluxes higher than 20-23 kW/m^2 to initiate the swelling process [40]. Consequently, the swelling rate of the intumescent coating was assumed null for incident heat fluxes lower than this critical incident heat flux for the onset of swelling. As a result, the swelling rate of the intumescent coating $\dot{d}_c$ [mm/min] can be expressed as a function of the incident heat flux $\dot{q}''_{inc}$:

$$\dot{d}_c = \begin{cases} 0 & \text{if } \dot{q}''_{inc} < 20 \text{ kW/m}^2 \\ -0.0001(\dot{q}''_{inc})^2 + 0.0280 \cdot \dot{q}''_{inc} - 0.3320 & \text{if } \dot{q}''_{inc} \geq 20 \text{ kW/m}^2 \end{cases} \quad (2)$$

In conclusion, the evolution of the swelled thickness of the intumescent coating $d_c(t)$ [mm] during thermal exposure can be estimated using the following expression:

$$d_c(t) = \begin{cases} DFT + \dot{d}_c \Delta t & \text{if } DFT + \dot{d}_c \Delta t < d_{max} \\ d_{max} & \text{if } DFT + \dot{d}_c \Delta t \geq d_{max} \end{cases} \quad (3)$$

where d_{max} is the maximum swelled coating thickness [mm], DFT is the applied initial dry film thickness [mm], $d_c(t)$ is the swelled coating thickness at the time increment Δt [mm], Δt is the time increment (from the beginning of the thermal exposure) [min] and $\dot{q}''_{inc}$ is the constant incident heat flux [kW/m^2]. For simplicity, the swelling rate was linearised during the whole thermal exposure: the onset of swelling was considered at time zero (at the application of the external heat flux), and the swelling rate was considered constant. The time to onset of swelling was not included due to its minor influence on the whole heat transfer problem (only a few minutes in the cases which registered significant swelling).

2.4 Definition of the material properties

The proposed heat transfer model assumes that the insulating effectiveness of the intumescent coating is mainly governed by its ability to develop swelled porous char [16]. Consequently, the thermo-physical properties of the intumescent coating, especially the ones of the swelled porous char, have a secondary role compared to the swelling process and the resulting swelled coating thickness. In addition, the experimental study has evidenced that the intumescent porous chars obtained from different experimental conditions have similar thermo-physical properties. This was also confirmed by the experimental results obtained using techniques aimed at estimating the thermal transport properties of the intumescent porous char: Transient Plane Source (TPS) and Laser Flash Analysis (LFA) equipment [38, 45-46]. Thus, the material properties of the intumescent coating used in the current heat transfer model were defined based on these experimental outcomes. For simplicity, the swelling intumescent coating is directly approximated as swelled porous char with constant material properties. Defining precise temperature-dependent material properties can increase the accuracy of the heat transfer model. However, since the problem is primarily controlled by the swelling process,

the heat transfer model is simplified to offer a solution characterised by a few governing parameters (lower complexity).

Following the outcomes from the described experimental studies [16, 38, 40], the thermal and physical properties of the intumescent coating were defined as:

- Thermal conductivity: λ_c = 0.16 W/mK
- Density: ρ_c= 50 kg/m^3
- Specific heat capacity: $c_{p,c}(T)$ = 1550 J/kgK
- Absorptivity/Emissivity: $\alpha_c = \varepsilon_c$ = 0.90

In particular, each material property of the swelled coating char was estimated differently. The thermal conductivity was defined based on sensitivity analysis discussed in Section 4: using the steady-state value measured using traditional thermal transport methodologies (TPS and LFA [38, 45-46]) would have increased the model error. The density was evaluated by simple mass/volume measurements on the swelled porous chars obtained from the bench-scale experiments [16, 38]. The specific heat capacity was determined based on the experimental results on the thermal transport properties of the intumescent coating at ambient and elevated temperatures using TPS and LFA techniques [38, 40, 45-46]. Finally, the coating absorptivity/emissivity was calculated as the average value within the 0.86-0.93 range evaluated using the Integrating Sphere System (ISS) [38, 40, 47]. The proposed material properties do not correspond to exact values, but they are lumped into effective properties that enable an accurate estimation of the thermal and physical evolution of the tested samples under specific conditions. In particular, the thermal conductivity of the swelled porous char can undergo an optimisation process to increase the model estimation under multiple scenarios, presented in Section 4. In the same section, the implications of adopting these material properties and the sensitivity of the proposed heat transfer model to these parameters are also discussed.

Lastly, with regards to the steel substrate, the thermal and physical properties of carbon steel were defined in accordance with Eurocode 3 [48]:

- Thermal conductivity: $\lambda_s(T)$ [W/mK] according to clause 3.4.1.3
- Density: ρ_s= 7850 kg/m^3
- Specific heat capacity: $c_{p,s}(T)$[J/kgK] according to clause 3.4.1.2

3 MODELLING RESULTS AND EXPERIMENTAL COMPARISON

The numerical model was implemented to solve the heat transfer problem for all the experimental cases reported in [16]: six different constant incident heat fluxes (10, 25, 40, 50, 70 and 90 kW/m^2)

and three different applied initial DFTs (*ñ L o w DFT ò*, *ñ M e d i u m DFT ò*, and *ñ H i g h DFT ò*). The main modelling results are presented and commented on in the following sections. Comparisons with other classical models for intumescent coatings mentioned in Section 1 are not possible because of the model's definition and input parameters. The proposed model is based on the accurate thermal and physical characterisation of the swelling intumescent coating during thermal exposure (i.e. substrate conditions, thermal boundary conditions at the coating surface, and swelled coating thickness), and all this information is rarely quantified and reported in classical studies in the available literature.

3.1 Swelled coating thickness

The evolution of the swelled thickness of the tested intumescent coating during thermal exposure can be calculated using Equation 1, Equation 2, and Equation 3. In accordance with the measured mean DFTs for the three groups of test samples, the initial thickness of the intumescent coating was set equal to 1.0 mm, 1.8 mm or 2.9 mm for *ñLow DFTò*, *ñMedium DFTò* or *ñHigh DFTò*, respectively. Figure 5 compares the experimentally-measured swelled coating thickness, and the one estimated using the described empirical correlations for a sample set of experiments (50 kW/m^2). As can be seen, the model is capable of estimating the trends but it occasionally under- or over-estimates the swelled coating thickness. The same trend was observed for all other experiments. The implications of adopting the described empirical correlations are discussed in detail in the sensitivity analysis presented in Section 4.

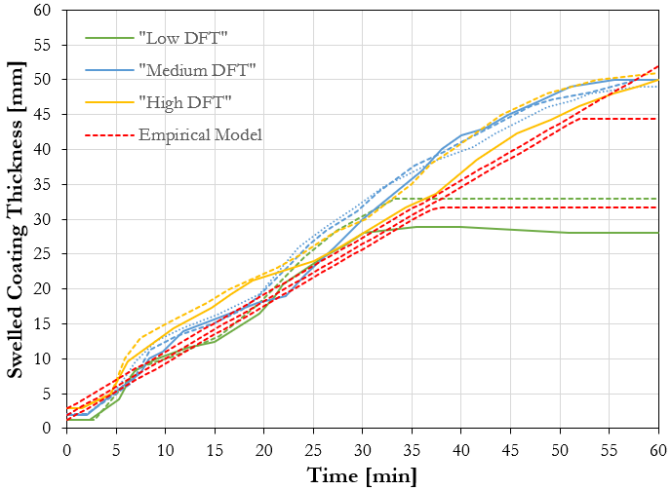

Figure 5. Comparison between the evolution of the experimentally-measured swelled coating thickness and the one estimated using empirical correlations (50 kW/m^2, different applied initial DFTs).

3.2 Coating surface and substrate temperatures

Once assessed the evolution of the swelled coating thickness during thermal exposure, the analysis investigates the two extremes of the thermal gradient within the swelling intumescent coating: the

coating surface temperature and the steel substrate temperature. Figure 6 compares the evolution of the experimentally-measured coating surface and steel substrate temperatures to the ones estimated using the described heat transfer model for a sample set of experiments (50 kW/m^2, ñ *Me d i u m*). *D F T ò* Regarding the steel substrate, similarly to the swelled coating thickness, the model is capable of estimating the trends but it occasionally under- or over-estimates the steel temperature. The same trend was observed for all other experiments. However, the discrepancy between the experimental and modelled temperatures is directly related to the definition of the thermal conductivity of the intumescent coating, discussed in detail in the sensitivity analysis presented in Section 4.

The experimental surface temperature is reported as the envelope of the measured temperatures at the coating surface evaluated by post-processing the data obtained by an Infra-Red camera: averaged over the central area of the test sample and the envelopes were obtained from a sensitivity analysis on the coating emissivity (maximum values: $\varepsilon = 0.85$; minimum values: $\varepsilon = 0.95$) [16, 38]. In general, the surface temperature trend is captured, but the surface temperatures are generally underestimated. This could be related to different aspects. The first reason could be related to oxidation taking place at the coating surface in the oxygen-rich environment of the H-TRIS test method. The available literature underlines how, in the presence of oxygen and at temperatures above 550°C, the intumescent coating undergoes oxidation reactions [16, 38]. Since the proposed model does not consider any oxidation process, the surface temperature may be under-estimated. Another reason could be related to the accuracy of the imposed thermal boundary conditions: the constant incident heat flux at the sample surface was applied with an accuracy of ± 10% [16, 38]. Moreover, the estimated surface temperature and the surface temperature measured using the IR camera strongly rely on a correct definition of the surface properties of the intumescent coating, especially absorptivity and emissivity [16, 38]. These parameters control the net heat flux received by the test samples by defining the absorbed heat by the intumescent coating and the radiation losses at the coating surface. The current model employs a constant average value (0.90), independent of the material temperature and the radiation wavelength. This assumption may be another potential cause of deviation between the experimental and the modelled cases. Lastly, since the intumescent coating is immediately modelled as swelled porous char with highly-insulating properties and no transient phenomena (from virgin coating towards swelling coating and swelled porous char) are considered in the model, the proposed model poorly estimates the initial transient phase of the heat transfer problem. In this phase, the intumescent coating gradually increases its surface temperature and commences the swelling process. Since this phase is more rapid for high heat fluxes, this under-estimation is more evident for low heat fluxes.

In general, the heat transfer model can describe the heat transfer within the swelling intumescent coating because it restricts the problem by defining the two edges of the thermal gradient. The thermal gradient within the intumescent coating is mainly governed by the swelled coating thickness and the thermal boundary conditions at the coating surface. The surface coating temperature depends on the heating conditions, and the coating swelling stretches the thermal gradient between the steel substrate and the coating surface [16, 38]. It is noteworthy that applying the numerical model to the case of 10 kW/m^2, along with all the cases that do not trigger the swelling of the intumescent coating, loses relevance. In these cases, the heat transfer problem is primarily transient and other models such as the one proposed for conditions prior to the onset of swelling [40] represents a preferable option.

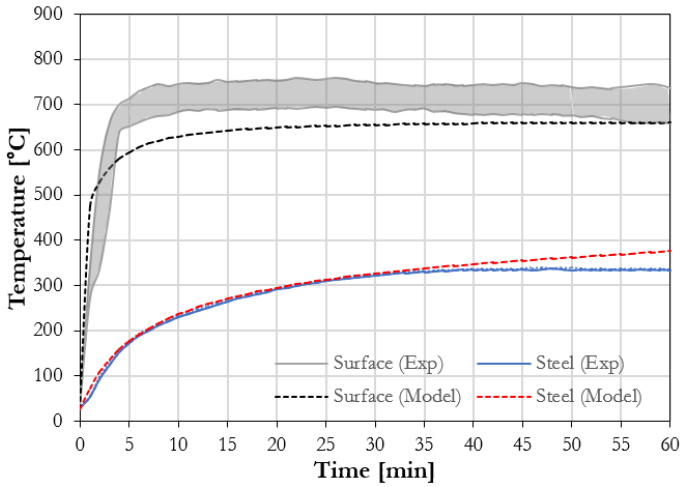

Figure 6. Comparison between the experimentally-measured coating surface and steel temperatures and the ones estimated using the described heat transfer model (50 kW/m^2, ñ *Me d i u m*). *D F T ò*

3.3 Coating in-depth temperatures

Using the experimental measurements and adopting the described heat transfer model, it is also possible to investigate the evolution of the in-depth temperature profiles within the swelling coating during thermal exposure. Figure 7 reports the comparison between the experimentally-measured and estimated in-depth temperature profiles for a sample set of experiments (50 kW/m^2, ñ *Me d i u m*). *D F T ò* For neatness of graphical visualisation, three instants during the thermal exposure were selected and plotted: 10, 30 and 60 minutes. Furthermore, the graphs only report the average in-depth temperature profile, evaluated between different experimental repetitions: all the different temperature curves are available in [38]. In Figure 7, the accuracy of each experimental measurement was provided using error bars at the last data point (coating surface). The horizontal error bars represent the accuracy of the location of the in-depth thermocouple and the evaluation of the swelled thickness of the intumescent coating (± 2 mm) [16, 38]. On the other hand, the vertical error bars represent the

accuracy of the surface coating temperature and the maximum temperature discrepancy between different experimental repetitions [16, 38].

The first significant characteristic of the in-depth temperature profiles obtained from the numerical model is their linearity. Common heat transfer problems of insulation materials (high Biot number) with well-defined thermal properties and constant geometrical dimensions (e.g. thickness) are usually constituted by a transient phase and a steady-state phase [42]. At the beginning of any thermal exposure, the transient phase is generally characterised by a curved in-depth thermal profile due to transient phenomena (e.g. heat capacitance vs thermal conduction) occurring within the insulation material. Successively, the in-depth temperature profile gradually tends to equilibrium, characterised by a linear gradient according to the thermo-physical properties and the thermal boundary conditions of the insulation material (if constant). However, based on the assumptions and the definition of the heat transfer problem, this case is essentially different. As highlighted in the definition of the coating properties within the current study, the modelling of swelling intumescent coatings becomes a physical problem, mainly driven by the definition of the swelled coating thickness. The heat transfer problem is actually quasi-steady-state due to the highly-insulating material properties of the coating porous char, the applied constant incident heat flux and the relatively-high coating swelling rate, compared to the penetration speed of the heat wave within the intumescent coating. Following these assumptions, the duration of the transient phase is minimal, the coating surface quicky achieves thermal equilibrium with the external conditions, and a quasi-steady-state linear thermal gradient within the intumescent coating is obtained based on its swelled thickness.

Consequently, the discrepancy between the experimentally-measured and estimated in-depth temperature profiles is foreseeably more significant in the first part of the thermal exposure and for lower constant incident heat fluxes, hence the cases in which transient phenomena are more relevant. Despite the shape, the thermal gradient within the intumescent coating is generally captured. This is the direct consequence of a good estimation of the temperature evolutions at the coating surface and steel substrate.

In addition, it is important to stress that the in-depth temperatures obtained using K-type thermocouples are subjected to significant errors because of the measurement characteristics [16, 38]. Several researchers have highlighted how the in-depth measurements within a low-conductivity material may be significantly affected by the measuring methodology. In particular, the relatively big size of the used K-type thermocouples (1.5 mm diameter), the positioning of the in-depth thermocouples in parallel to the main direction of the heat transfer (from the rear of test samples) and the possible creation of an air-gap around the thermocouple head may have introduced considerable

errors to the in-depth temperature measurements [49-50]. The magnitude of the error is difficult to quantify, but it is important to acknowledge it for different applications or future studies. Nevertheless, the discussed in-depth thermocouple measurements do not constitute an input variable of the presented model, as a typical inverse heat conduction approach [51]. The model relies on the accurate definition of coating boundary conditions (i.e. surface, substrate, and DFT). Consequently, the large uncertainties associated with the in-depth thermocouple measurements do not have a direct effect on the modelling outcomes and, within this section, the coating in-depth temperatures are introduced only as a qualitative comparing parameter. Only the substrate temperature evolution (i.e. steel plate) has been used to benchmark the model accuracy and these values are expected to have a much smaller error compared to in-depth measurements [49-50].

Another important point regarding the evolution of the in-depth temperature profiles is the presence of in-depth oxidation within the swelling intumescent coating, typically observed for high heat fluxes [38]. As already discussed, the adopted heat transfer model disregards this phenomenon due to its high complexity, and this topic falls outside the scope of this research study.

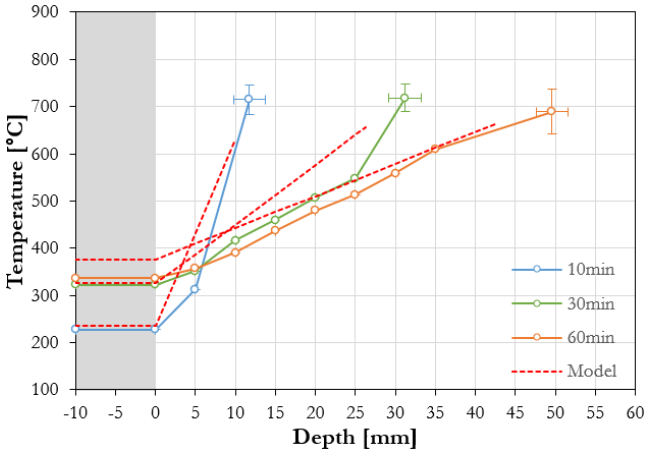

Figure 7. Comparison between the experimentally-measured in-depth temperature profiles (steel and coating) and the ones estimated using the described heat transfer model at different instants during the heating exposure(50 kW/m^2, ñ *Me d i u m*). *D F T* ò

4 SENSITIVITY ANALYSIS

The accuracy of the numerical model was verified through a sensitivity analysis to some key governing factors embedded in the model assumptions. The sensitivity analysis investigates the influence of uncertainty in certain key parameters on the modelling results for a sample set of experiments. In particular, this analysis focuses on the implications of the definition of the material properties of the intumescent coating, the surface thermal boundary conditions (i.e. incident heat flux), the initial coating thickness (DFT) and the adopted empirical correlations for calculating the swelling rate of the intumescent coating.

The model accuracy was evaluated based on the Root-Mean-Square Error (RMSE) between the experimentally-measured temperature evolution of coated steel plates ($T_{s,exp}$) compared to the estimated one using the described heat transfer model ($T_{s,mod}$), evaluated at 1 min time-intervals:

$$RMSE(T_s) = \pm\sqrt{\frac{\sum\left(T_{s,exp} - T_{s,mod}\right)^2}{N}} \quad (4)$$

The model was benchmarked against the temperature evolution of the coated steel plate because the substrate temperature represents the main performance criteria for most applications in fire safety engineering. In each case, a sign was given to the Root-Mean- Square Error (RMSE) to record if the model under- or over-estimates the experimental measurements. Positive RMSE represents a model over-estimation, while a negative RMSE an under-estimation.

4.1 Coating material properties

Since the proposed model is mainly based on heat conduction, the sensitivity and uncertainty analysis first focuses on understanding the relevance of each single thermal and physical property defined in the heat transfer problem and described in Section 2.4. This analysis is mainly carried out on the material properties of coating porous chars. The same analysis on the material properties of steel has minor importance, considering that the steel properties are well-defined and have a minimal uncertainty, particularly for temperatures below 500°C [48].

Figure 8 reports the results obtained from the sensitivity analysis with respect to the thermal conductivity, density, specific heat capacity and absorptivity/emissivity of the intumescent coating for different incident heat fluxes and the ñ Me di um exemplar case. The sensitivity analysis revealed clear trends. The density, the specific heat capacity and the absorptivity/emissivity of the intumescent coating have a minor influence on the accuracy of the heat transfer model, while the thermal conductivity plays a key role. This outcome was expected as the problem can be described as a quasi-steady state conduction heat transfer problem, where the volumetric heat capacity plays a minor role. As already highlighted by the in-depth temperature profiles, given its characteristics, the model focuses on solving a quasi-steady-state heat transfer problem and the transient thermal states dominated by the kinetics of the reaction are overlooked.

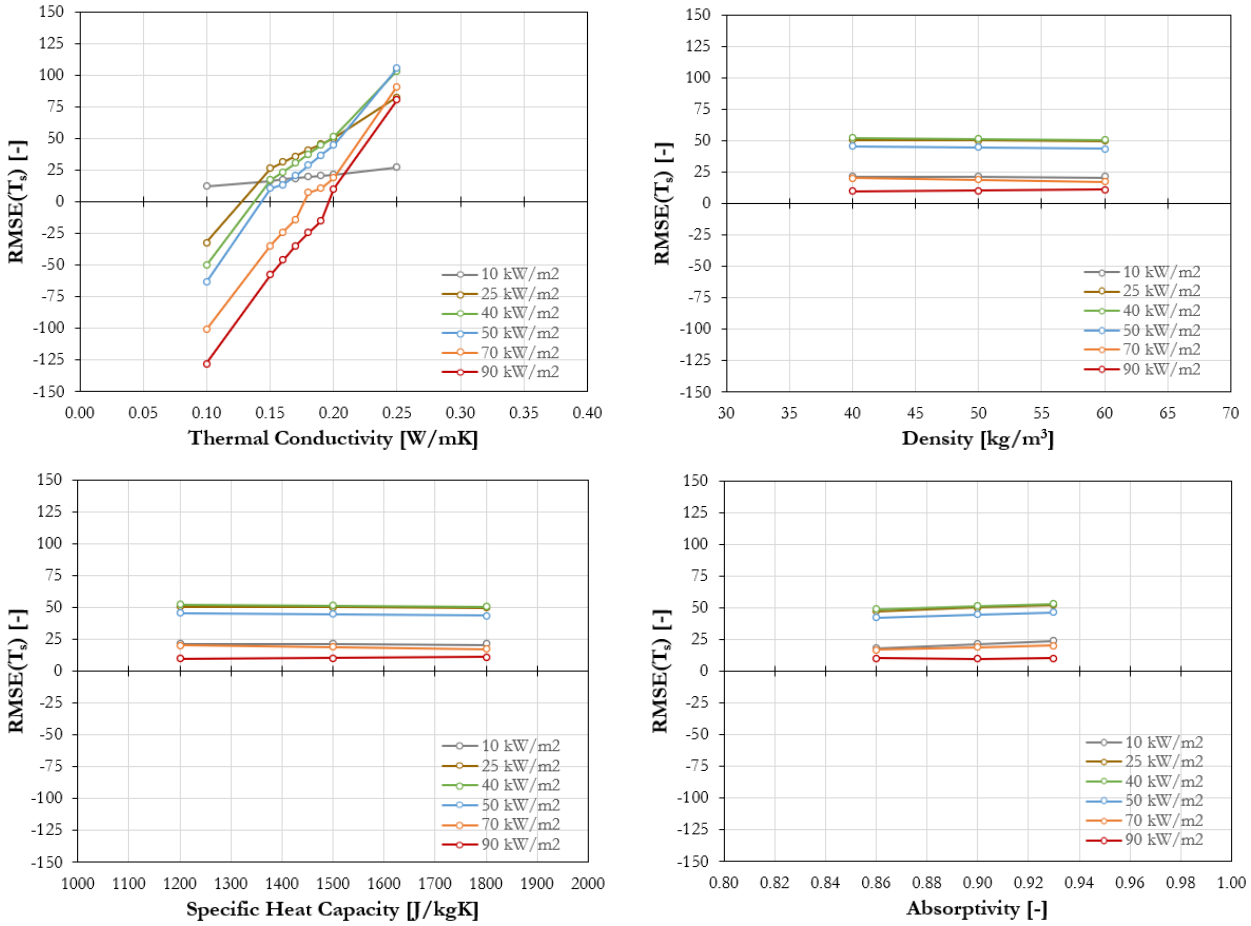

Figure 8. Sensitivity analysis with respect to the thermal conductivity, density, specific heat capacity and absorptivity/emissivity of the intumescent coating (*ñMedium DFT*").

Specific attention was paid to the definition of the constant thermal conductivity of the swelled porous char described in Section 2.4 and this parameter was subjected to an optimisation process. As highlighted in Figure 8, no specific value of the thermal conductivity is able to eliminate the discrepancy (zero deviation) between the model and the experimental measurements for all the examined conditions. A similar trend was observed for the different heating conditions, except for 10 kW/m^2 (fundamentally different), and for the different initial thicknesses, *ñLow DFTò* and *ñHigh DFTò* (not presented here). In order to quantify the minimum discrepancy, the total Root-Mean-Square Error $\sum RMSE(T_s)$ between the experimentally-measured and estimated temperature evolutions of coated steel plates was calculated as the sum of RMSE absolute values for all the different heating conditions. Figure 9 displays the results obtained from this analysis, separately carried out for the different DFTs. The values of thermal conductivity that produced the minimum total error were 0.16 W/mK for *ñ Medium DFTò*, and 0.17 W/mK for *ñ Low DFTò*. Therefore, the thermal conductivity of the intumescent coating λ_c was set equal to 0.16 W/mK.

Adding or removing the deviation related to the case of 10 kW/m^2 was marginal due to the different fundamental nature of the problem (no swelling).

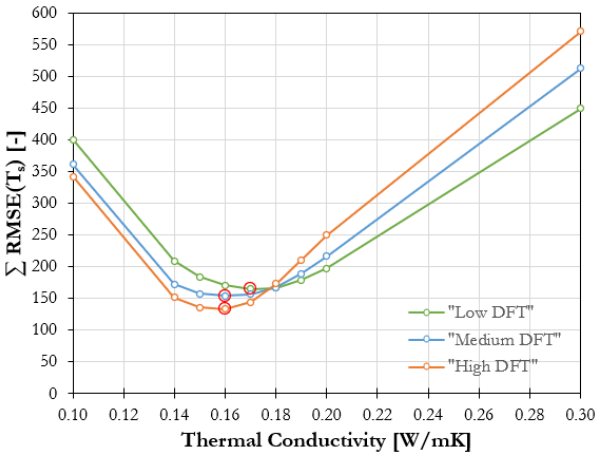

Figure 9. Total Root-Mean-Square Error (RMSE) for different thermal conductivity values of the intumescent coating.

This definition of the thermal conductivity of the intumescent coating implies that the error throughout the whole problem is minimised, and the model-experiments discrepancy is balanced between over- and under-estimated cases. Figure 10 highlights how the steel temperatures are generally over-estimated (positive RMSE) for lower heat fluxes, while they are under-estimated (negative RMSE) for higher heat fluxes. In general, the numerical model has good accuracy in solving the heat transfer problem. However, within the structural fire safety engineering practice, an under-estimation of the steel temperatures may imply a potential failure on the unsafe side. Optimisation processes for the definition of the thermal conductivity of the intumescent coating, similar to the one presented herein, could be implemented to consistently estimate the steel temperatures on the safe side (over-estimation, positive RMSE). For instance, this process was repeated for a value of thermal conductivity equal to 0.20 W/mK and the model deviations are reported in Figure 11.

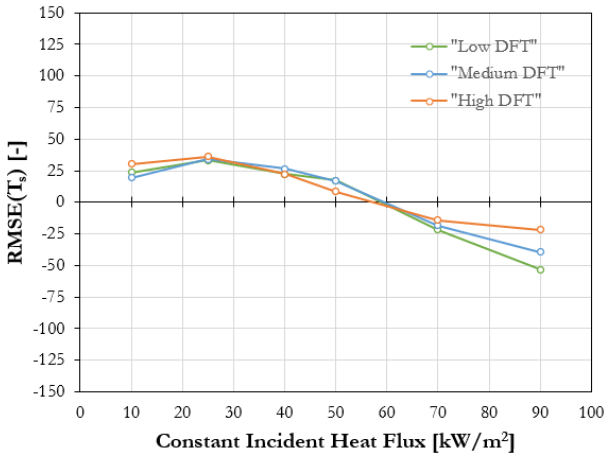

Figure 10. Root-Mean-Square Error (RMSE) for different constant incident heat fluxes and applied initial DFTs (λ_c = 0.16 W/mK).

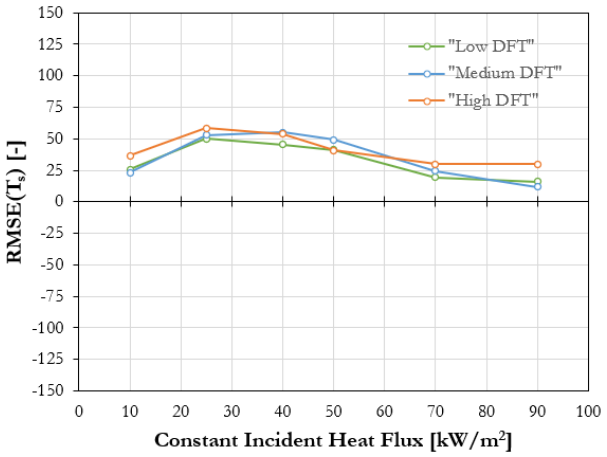

Figure 11. Root-Mean-Square Error (RMSE) for different constant incident heat fluxes and applied initial DFTs (λ_c = 0.20 W/mK).

4.2 Surface thermal boundary conditions (incident heat flux)

The experimental setup based on the radiant exposure of the H-TRIS test method reports that the distribution of the incident heat flux on the sample surface had an accuracy of ± 10% [16, 38]. In this analysis, the heating conditions of a constant incident heat flux of 50 kW/m^2 and an applied initial thickness ñ *M e d i u m* were chosen as general exemplar case. Therefore, in the case of 50 kW/m^2, an accuracy of ± 5 kW/m^2. Within the heat transfer model, the incident heat flux has a key role in the definition of the heating conditions because it is the heat transfer governing force and it defines the swelling rate of the intumescent coating (refer to Section 2.3). Figure 12 shows how the incident heat flux accuracy has a minimal influence on the evolution of the swelled coating thickness, but the resulting steel temperatures are practically identical. In conclusion, the numerical model appears to be robust with respect to the incident heat flux.

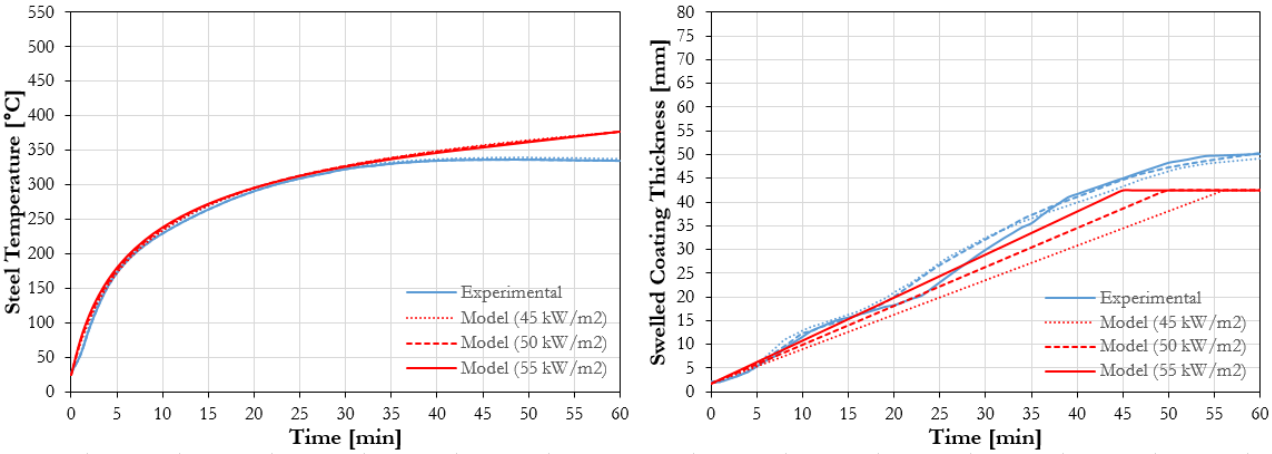

Figure 12. Sensitivity analysis with respect to the incident heat flux (50 kW/m^2, *"Medium DFT"*).

4.3 *Initial coating thickness (DFT)*

In the experiments on coated steel plates, the test samples were categorised into three DFT groups with an accuracy of ± 0.20 mm [16, 38]. In the case of *"Medium"* (1.80 mm), the average DFT of the test samples was included in the range between 1.60 mm and 2.00 mm. Within the defined heat transfer model, the initial thickness governs the maximum swelled thickness that the intumescent coating can achieve during the thermal exposure (refer to Section 2.3). Figure 13 shows how the maximum swelled coating thickness slightly changes depending on the accuracy of the initial coating DFT, but the resulting steel temperatures are only slightly affected (± 10°C). In conclusion, as for the case of the incident heat flux, the numerical model appears to be robust concerning the applied initial coating DFT.

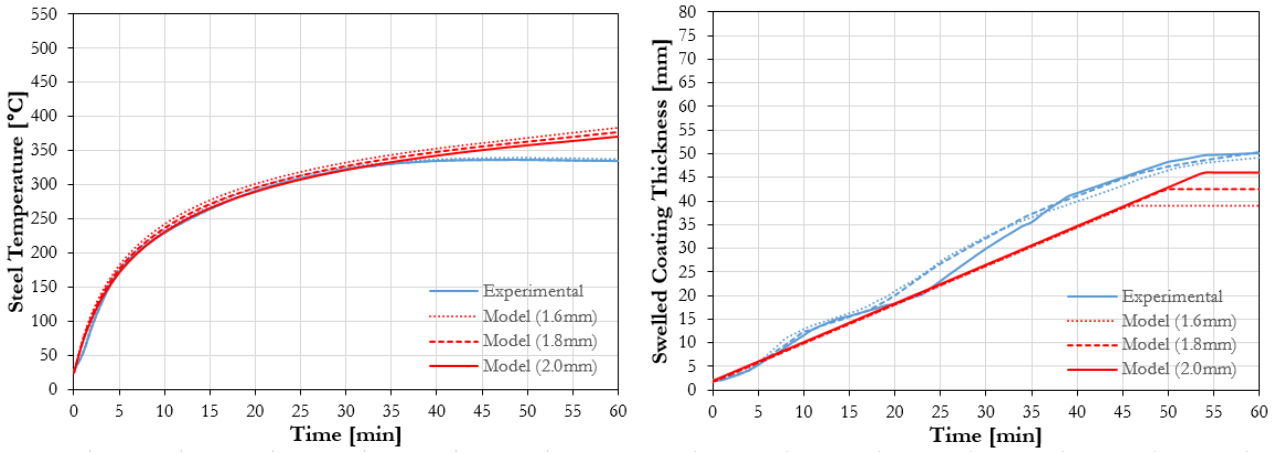

Figure 13. Sensitivity analysis with respect to the applied initial DFT (50 kW/m^2, *"Medium DFT"*).

4.4 *Coating swelling rate*

Lastly, the different experimental repetitions highlighted that, within the same heating conditions, the coating swelling rate of the intumescent coating was included within a certain range, defined by an upper and lower bound (see Figure 4). In the case of 50 kW/m^2, swelling rates between 0.78 mm/min (lower bound) and 0.96 mm/min (upper bound) were measured. However, Equation 2 defined a unique value equal to 0.82 mm/min. Figure 14 shows how the modelling results are influenced by the definition of the coating swelling rate. The evolution of the swelled coating thickness has a slightly different slope (i.e. swelling rate), but the coating reaches the same final swelled thickness. However, this has a more important influence on the resulting steel temperature (± 30°C) compared to the external heat flux and initial coating thickness. In conclusion, the sensitivity analysis underlined how the heat transfer model is particularly sensitive to the coating swelling rate, and it consequently requires a careful definition and treatment of it.

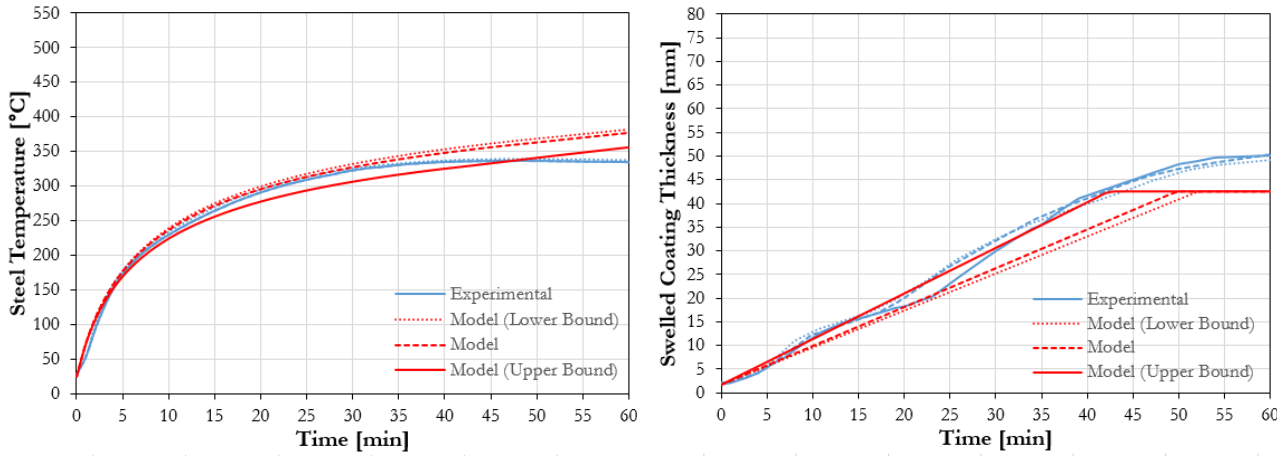

Figure 14. Sensitivity analysis with respect to the swelling rate (50 kW/m^2, *"Medium DFT"*).

4.5 Discussion

To better understand the influence of these parameters on the heat transfer problem, the sensitivity analysis for the incident heat flux, the applied initial DFT, and the swelling rate of the intumescent coating was extended for all the experimental heating conditions. Figure 15 offers an overview of how the three parameters affect the model convergence. The plots confirm that uncertainty in constant incident heat flux (± 10%) and the applied initial DFT (± 0.20 mm) has a minor effect. On the contrary, Figure 15 underlines how the heat transfer model is especially sensitive to the coating swelling rate. The discrepancy increases for higher incident heat fluxes, where a bigger scattering of the experimental swelling rates was registered (refer to Figure 4). In conclusion, this sensitivity analysis stresses the importance of carefully estimating the swelling rate and swelled coating thickness, which are the main governing factors of the effectiveness of intumescent coatings.

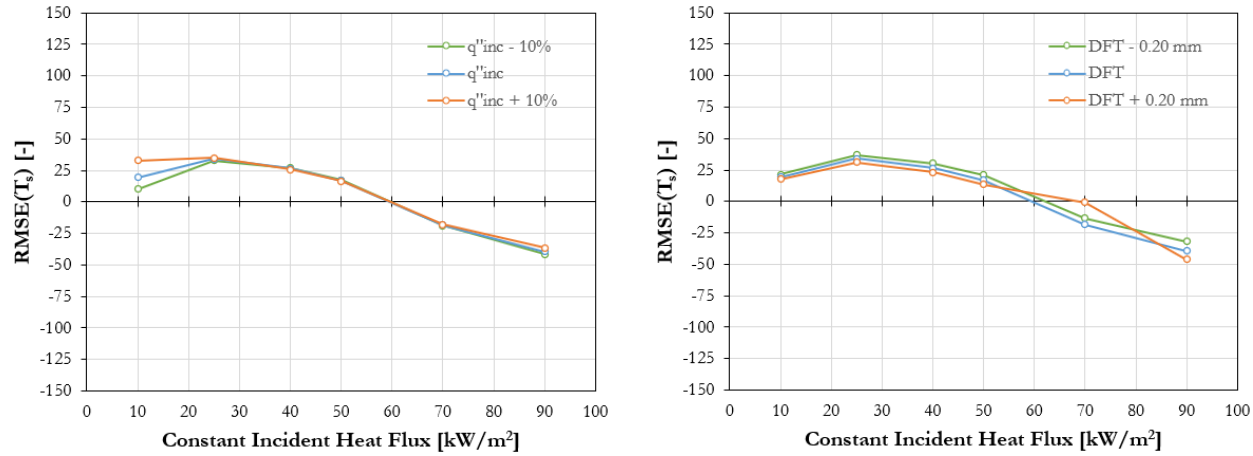

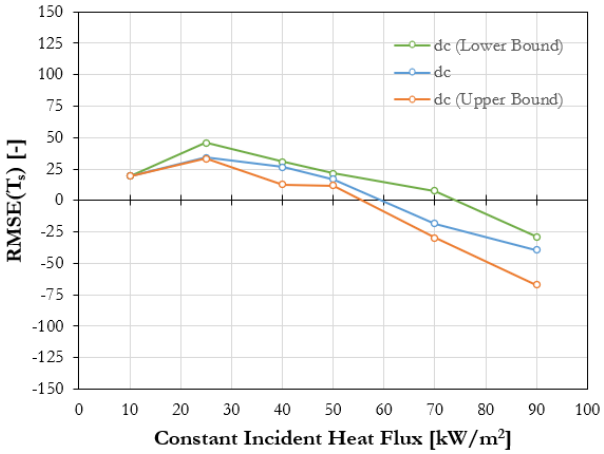

Figure 15. Sensitivity analysis with respect to the incident heat flux, the applied initial DFT and the swelling rate of the intumescent coating for different constant incident heat fluxes (*"Medium DFT"*).

5 CONCLUSIONS

The modelling study presented herein proposes a heat transfer model aimed at estimating the thermal and physical behaviour of intumescent coatings under thermal exposure. The heat transfer model is formulated based on the experimental outcomes obtained by testing steel plates coated with a commercial solvent-based intumescent coating for a range of constant incident radiant heat fluxes and initial coating thickness using the Heat-Transfer Inducing System (H-TRIS) test method. The model solves the one-dimensional heat conduction problem by resolving the energy conservation equation adopting the finite-difference Crank-Nicolson method. As per the experimental outcomes, the model assumes that the effectiveness of the thermal barrier provided by the intumescent coating is mainly dependent on the ability to develop swelled porous char, defined with specific constant material properties. The swelling of the intumescent coating is implemented by adopting a novel approach based on adding finite elements in proximity of the substrate-coating interface, where the swelling process takes place and insulates the protected substrate by displacing the already-swelled coating char towards the direction of the heat source. Empirical correlations based on the well-defined thermal conditions at the coating boundaries and the applied initial coating thickness are introduced to estimate the evolution of the swelled coating thickness during exposure to a constant heat flux.

From the results obtained from the heat transfer model, the following concluding remarks can be drawn:

- The insulating performance and effectiveness of intumescent coatings are mainly governed by the swelling process and the resulting swelled coating thickness. Sensitivity analyses underlined how the heat transfer becomes a physical problem. The model accuracy is primarily dependent on the correct estimation of the evolution of the swelled coating thickness

(i.e. swelling rate). On the contrary, the thermo-physical properties of the intumescent porous char have a secondary role.

- The heat transfer model is capable of characterising the heat transfer through swelling intumescent coatings by estimated the evolution of coating surface and substrate steel temperatures, and the evolution of the swelled coating thickness. In this way, the thermal gradient within the swelling intumescent coating is correctly estimated, despite the profile shape. The estimation accuracy varied for different cases, and it can be adjusted following an optimisation process on the thermal conductivity of the intumescent coating.
- Based on the model assumptions and simplifications, the formulated model defines a quasi-steady-state thermal problem. The highly-insulating swelled coating acts as thermally-thick material rapidly, achieving a quasi-steady surface temperature in equilibrium with the constant incident heat flux (high Biot number). Consequently, the duration of transient phases and transient phenomena are minimised, and linear thermal gradients are obtained.
- The heat transfer model is more accurate for conditions close to steady-state, for example, high heat fluxes, characterised by high swelling rates (high Biot number). On the contrary, the model loses accuracy for cases characterised by transient phenomena: phases prior to the onset of swelling (low Biot number) and low heat fluxes (longer transient phase and low swelling rates).

This study aims at building the principles for developing engineering methods for the performance-based design of steel structures protected by intumescent coatings, taking into account their effectiveness for a wide range of potential conditions (e.g. fire scenarios or initial coating thickness). This research provides an essential modelling procedure applicable to any intumescent coating and testing conditions, if the necessary information can be extrapolated (e.g. swelled coating thickness and swelling rate). The results are therefore useful examples of the key information that can be extracted following the presented modelling approach. In that sense, this research study should remain product-independent and the specific coating just an example of application. Nevertheless, considering the wide variety of products available in the market and various possibilities to assess the fire behaviour of intumescent coatings, many input parameters, like the coating swelling rate and material properties, could be case-specific, and they could depend on large range of variables, such as the experimental setup and the intumescent formulation. Similar experimental and modelling campaigns should be performed under different conditions to comprehend if the presented research outcomes can be generalised. In addition, the modelling approach presented herein is only valid for constant external heat fluxes; its accuracy for transient external heat fluxes is yet to be studied.

ACKNOWLEDGEMENTS

The authors would like to gratefully acknowledge the scientific and technical support kindly offered by the Fire Safety Engineering Research Group at The University of Queensland, in particular Jeronimo Carrascal Tirado and Stewart Matthews. The authors would also like to thank all BEng-MEng and PhD students, academics, professionals, researchers, and technical staff who collaborated on the research projects related to intumescent coatings and led by Dr Andrea Lucherini. The authors are also grateful for the collaboration and continuous support kindly offered by Remedial Building Services Australia Pty Ltd, especially Qazi Samia Razzaque, Edward Kwok, Long Le and Andrew Abrahams.

CREDIT AUTHOR STATEMENT

Andrea Lucherini: Conceptualization, Data Curation, Formal Analysis, Investigation, Methodology, Resources, Writing - Original Draft; **Juan P. Hidalgo**: Conceptualization, Supervision, Writing - Review & Editing; **Jose L. Torero**: Conceptualization, Supervision, Writing - Review & Editing; **Cristian Maluk**: Conceptualization, Supervision, Writing - Review & Editing.

REFERENCES

[1] Buchanan A.H., and Abu A.K. *Structural design for fire safety*. John Wiley & Sons, 2nd Edition, 2017. https://doi.org/10.1002/9781118700402

[2] Weil E.D. *Fire-protective and flame-retardant coatings – A state-of-the-art review*. Journal of Fire Science, vol. 29, pp. 259-296, 2011. https://doi.org/10.1177/0734904110395469

[3] Puri E.G., and Khanna A.S. *Intumescent coatings: a review*. Journal of Coatings Technology and Research, vol. 14, pp.1-20, 2017. https://doi.org/10.1007/s11998-016-9815-3

[4] Ghiji M., Joseph P., and Guerrieri M. *Some recent developments and testing strategies relating to the passive fire protection of concrete using intumescent coatings: a review*. Journal of Structural Fire Engineering, 2022. https://doi.org/10.1108/JSFE-11-2021-0069

[5] Lucherini A., Razzaque Q.S., and Maluk C. *Exploring the fire behaviour of intumescent coatings used*. Fire Safety Journal, vol. 109, pp. 102887, 2019. https://doi.org/10.1016/j.firesaf.2019.102887

[6] Mariappan T. *Recent developments of intumescent fire retardant coatings: A review*. Journal of Fire Sciences, vol. 34, no. 2, pp. 1-44, 2016. https://doi.org/10.1177/0734904115626720

[7] Lucherini A., and Maluk C. "Intumescent coating-based fire safety design of steel structures". Journal of Constructional Steel Research, vol. 162, n. 105712, 2019. https://doi.org/10.1016/j.jcsr.2019.105712

[8] Dreyer J.A.H., Weinell C.E., Dam-Johansen C., and Kill S. "Review of heat and in-situ characterisation techniques". Fire Safety Journal, vol. 121, no. 103264, 2021. https://doi.org/10.1016/j.firesaf.2020.103264

[9] Kolsek J., and Cesarek P. "Performance-based fire modelling of intumescent painted steel structures and". Journal of Constructional Steel Research, vol. 104, pp. 91-103, 2015. https://doi.org/10.1016/j.jcsr.2014.10.008

[10] Lucherini A., Giuliani L., and Jomaas G. "Experimental study of the coatings exposed to standard and non-standard fi". Fire Safety Journal, vol. 95, pp. 42-50, 2018. https://doi.org/10.1016/j.firesaf.2017.10.004

[11] Li G.Q., Lou G.B., Zhang C., Wang L., and Wang Y. "Assess the fire resis coatings by equivalent". Fire Technology, vol. 48, pp. 529-546, 2012. https://doi.org/10.1007/s10694-011-0243-8

[12] Wang L., Dong Y., Zhang D., Zhang D., and Zhang C. "Experimental study o intumescent coatings exposed to non-standard fu". Fire Technology, vol. 51, no. 1, pp. 627-643, 2015. https://doi.org/10.1007/s10694-015-0460-7

[13] Elliott A., Temple A., Maluk C., and Bisby L. "Novel testing to study intumescent coatings under non-standard he". Fire Safety Science—Proceedings of the 11th International Symposium, University of Canterbury, New Zealand, pp. 652-665, 2014. https://doi.org/10.3801/IAFSS.FSS.11-652

[14] Zhang Y., Wang Y., Bailey C.G., and Taylor A.P. "Global modelling of performances of an intumescent c". Journal of Fire unde Science, vol. 31, no.1, pp. 51-72, 2012. https://doi.org/10.1177/0734904112453566

[15] Zhang Y., Wang Y., Bailey C.G., and Taylor A.P. "Global modelling of performance of an intumescent coating .under". Fire Safety Journal, vol. 50, pp. 51-62, 2012. https://doi.org/10.1016/j.firesaf.2012.02.004

[16] Lucherini A., Hidalgo J.P., Torero J.L., and Maluk C. "Influence of heating thickness on the effectiv". Fire Safety Journal, vol. 120, no. 103078, 2021. https://doi.org/10.1016/j.firesaf.2020.103078

[17] Lucherini A., Torero J.L., and Maluk C. "Effects of substrate therm of thin intumes". Interflam 2019: Fire Resistance, Fire and Materials, pp. 1-14, 2020. https://doi.org/10.1002/fam.2840

[18] de Silva D., Bilotta A., and Nigro E. "*A approach for modelling thermal coating applied*". Fire Safety Journal, vol. 116, no. 103200, 2020. https://doi.org/10.1016/j.firesaf.2020.103200

[19] International Organization for Standardization (ISO). "*ISO-834, Fire resistance Tests - Elements of Building Construction - Part 1: General Requirements*" Geneva, Switzerland, 1999.

[20] Comité Européen de Normalisation (CEN). "*EN 13381-8, Fire resistance tests - Part 1: General Rules*". Brussels, Belgium, 2012.

[21] Comité Européen de Normalisation (CEN). "*EN 1-8, Test methods for determining the contribution to the fire resistance of structural members - Part 8: Applied reactive protection to steel members*". Brussels, Belgium, 2013.

[22] Yuan J. "*Intumescent coating performance on steel*". PhD thesis, School of Mechanical, Aerospace and Civil Engineering, University of Manchester, 2009. https://ethos.bl.uk/OrderDetails.do?uin=uk.bl.ethos.498956

[23] Staggs J.E.J., Crewe R.J., and Butler R. "*A theoretical and experimental intumescent behaviour in pro*". Chemical Engineering Science, vol. 71, pp. 239-251, 2012. https://doi.org/10.1016/j.ces.2011.12.010

[24] Griffin G.J. "*The modelling of heat transf*". Journal of Fire Science, vol. 28, pp. 249-277, 2010. https://doi.org/10.1177/0734904109346396

[25] Bourbigot S., Duquesne S., and Leroy J.-M. "*Modeling of heat transfer intumescent system*". Journal of Fire Sciences, vol. 17, pp. 42-56, 1999. https://doi.org/10.1177/073490419901700103

[26] Anderson C.E., Dziuk J., and Mallow W.A. "*Intumescent re*". Journal of Fire Sciences, vol.3, no. 3, pp. 161-194, 1985. https://doi.org/10.1177/073490418500300303

[27] Cagliostro D.E., Riccitello S.R., Clark K.L., and Shimizu A.B. "*Intumescent coati*". Journal of Fire and Flammability, vol. 6, pp. 205, 1975.

[28] Di Blasi C. "*Modeling the effects of high radiati*". Journal of Analytical and Applied Pyrolysis, vol. 71, pp. 721-737, 2004. https://doi.org/10.1016/j.jaap.2003.10.003

[29] Di Blasi C., and Branca C. "*Mathematical steady decomposition of he intumescent*". AIChE Journal, vol. 47, pp. 2359-2370, 2001. https://doi.org/10.1002/aic.690471020

[30] Li G.Q., Lou G.B., Zhang C., Wang L., and Wang Y. "Assess the fire resis coatings by equivalent. Fire Technology, vol. 48, pp. 529-546, 2012. https://doi.org/10.1007/s10694-011-0243-8

[31] Li G.Q., Han J., Lou G.B., and Wang Y.C. "Predicting intumescent c temperature in fire usi Thin-Walled Structures, vol. 98, pp. 177- 184, 2016. https://doi.org/10.1016/j.tws.2015.03.008

[32] Cirpici B.K., Wang Y.C., and Rogers B. "Assessment of the thermal coatings . i Fire Safety Jo vol. 81, pp. 74-84, 2016. https://doi.org/10.1016/j.firesaf.2016.01.011

[33] Bilotta A., De Silva D., and Nigro E. "Tests on intumescent paints steel s. Construction and Building Materials, vol. 121, pp. 410-422, 2016. https://doi.org/10.1016/j.conbuildmat.2016.05.144

[34] Nadjai A., Petrou K., Han S., and Ali F. "Performance of unprotecte beams in fi Construction and Building Materials, vol. 105, pp. 579-588, 2016. https://doi.org/10.1016/j.conbuildmat.2015.12.150

[35] Weisheim W., Schaumann P., Sander L., and Zehfuss J. "Numerical model for performance and the design of intumescent co Journal of Structural Fire Engineering, 2019. https://doi.org/10.1108/JSFE-01-2019-0004

[36] Maluk C., Bisby L., Krajcovic M., and Torero J.L. "A Heat Transfer Inducting System (H-TRIS) test method Fire Safety Journal, vol. 105, pp. 307-319, 2019. https://doi.org/10.1016/j.firesaf.2016.05.001

[37] Lucherini A., and Maluk C. "Novel test methods for studyi intumescen Proceedings of 2nd International Fire Safety Symposium (IFireSS), Napoli, Italy, pp. 565-572, 2017.

[38] Lucherini A. "Fundamentals of thin intumescent coatings". PhD thesis, School of Civil Engineering, The University of Queensland, 2020. https://doi.org/10.14264/uql.2020.1021

[39] Wang Z., Han E., and Ke W. "Effects of nanoparticle-reinforced and the anti-ageing properties of flame-retardant". Surface & Coatings Technology, vol. 200, pp. 5706-5716, 2006. https://doi.org/10.1016/j.surfcoat.2005.08.102

[40] Lucherini A., and Maluk C. "Assessing the onset of swelling a range of heat Fire Safety Journal, vol. 106, pp. 1-12, 2019. https://doi.org/10.1016/j.firesaf.2019.03.014

[41] Lucherini A., Lam H.Y., Jimenez M., Samyn F., Bourbigot S., and Maluk C. *Fire test intumescent coatings: comparison between bench-scale furnace and radiant panels experimental method*. Fire Technology, In press, 2022.

[42] Incropera F.P., DeWitt D.P., Bergman T.L., and Lavine A.S. *Fundamental of heat transfer*. John Wiley & Sons, 6th Edition, 2006.

[43] Crank J., and Nicolson P. *A practical method for numerical differential equations of the heat-conduction*. Advances in Computational Mathematics, vol. 6, pp. 207-226, 1996. https://doi.org/10.1017/S0305004100023197

[44] Hidalgo J.P. *Performance-based methodology for the fire safe design of insulation materials in energy efficient*. PhD thesis, School of Engineering, The University of Edinburgh, 2015. http://hdl.handle.net/1842/10601

[45] International Organization for Standardization (ISO). *ISO 22007-2:2015 Plastics — Determination of thermal conductivity and thermal diffusivity - Part 2: Transient plane heat source (hot disk)*. Geneva, Switzerland, 2015.

[46] International Organization for Standardization (ISO). *ISO 22007-4:2008 Plastics — Determination of thermal conductivity and thermal diffusivity - Part 4: Laser flash*. Geneva, Switzerland, 2008.

[47] Seifter A., Grover M., Holtkamp D.B., Iverson A.J., Stevens G.D., Turley W.D., Veeser L.R., Wilke M.D., and Young J.A. *Emissivity measurement-wavelength shock integration*. Journal of Applied Physics, vol. 110, no. 093508, 2011. https://doi.org/10.1063/1.3656429

[48] Comité Européen de Normalisation (CEN). *EN 1993-1-2,9 Eurocode 3: Design of steel structures - Part 1-2: General rules - Structural*. Brussels, Belgium, 2005.

[49] Beck J.V. *Thermocouple temperature dist*. Journal of Heat Transfer, vol. 84, pp. 124-132, 1962. https://doi.org/10.1115/1.3684310

[50] Pope I., Hidalgo J.P., and Torero J.L. *A correction method for thermocouples in a low-conductivity c*. Fire Safety Journal, vol. 120, no. 103077, 2021. https://doi.org/10.1016/j.firesaf.2020.103077

[51] Bozzoli F., Mocerino A., Rainieri S. and Vocale P. *"Inverse heat transfer modeling applied to the estimation of the apparent thermal conductivity of an intumescent fire retardant paint"*. Experimental Thermal and Fluid Science, vol. 90, pp. 143-152, 2018. https://doi.org/10.1016/j.expthermflusci.2017.09.006